

# Coordinate Development of Skin Cells and Cutaneous Sensory Axons in Zebrafish

Georgeann S. O'Brien\*,<sup>1</sup> Sandra Rieger,<sup>1</sup> Fang Wang,<sup>1</sup> Gromoslaw A. Smolen,<sup>2</sup> Robert E. Gonzalez,<sup>1</sup> JoAnn Buchanan,<sup>3\*</sup> and Alvaro Sagasti<sup>1\*</sup>

<sup>1</sup>Department of Molecular, Cell and Developmental Biology, University of California, Los Angeles, California 90095

<sup>2</sup>Agios Pharmaceuticals, Cambridge, Massachusetts 02139

<sup>3</sup>Department of Molecular and Cellular Physiology, Stanford University, Stanford, California 94305

## ABSTRACT

Peripheral sensory axons innervate the epidermis early in embryogenesis to detect touch stimuli. To characterize the time course of cutaneous innervation and the nature of interactions between sensory axons and skin cells at early developmental stages, we conducted a detailed analysis of cutaneous innervation in the head, trunk, and tail of zebrafish embryos and larvae from 18 to 78 hours postfertilization. This analysis combined live imaging of fish expressing transgenes that highlight sensory neurons and skin cells, transmission electron microscopy (TEM), and serial scanning electron microscopy (sSEM). In zebrafish, the skin initially consists of

two epithelial layers, and all of the axons in the first wave of innervation are free endings. Maturation of the epithelium coincides with, but does not depend on, its innervation by peripheral sensory axons. We found that peripheral axons initially arborize between the two epithelial skin layers, but not within the basal lamina, as occurs in other organisms. Strikingly, as development proceeds, axons become tightly enveloped within basal keratinocytes, an arrangement suggesting that keratinocytes may serve structural or functional roles, akin to Schwann cells, in somatosensation mediated by these sensory neurons. *J. Comp. Neurol.* 520:816–831, 2012.

© 2011 Wiley Periodicals, Inc.

**INDEXING TERMS:** zebrafish; somatosensation; skin; peripheral axon; trigeminal; Rohon-Beard neurons

Our ability to sense mechanical, thermal, and chemical touch stimuli relies on the growth and development not only of the neurons that form somatosensory circuits but also of the skin, the site at which stimuli are detected. In all vertebrates, somatosensation is accomplished by trigeminal neurons, which innervate the head, and dorsal root ganglia (DRG) neurons, which innervate the body. In fish and amphibians, an additional population, Rohon-Beard (RB) neurons, innervates the trunk and tail during embryonic and early larval stages, before dying and being replaced by DRG neurons (see, e.g., Kimmel and Westerfield, 1990; Reyes et al., 2004). The cell bodies of trigeminal and DRG neurons cluster in ganglia outside the central nervous system (CNS), whereas RB neurons are located in the dorsal spinal cord (Fig. 1A). All three populations of somatosensory neurons share a common bipolar or pseudounipolar structure, projecting a central axon into the CNS that synapses onto downstream interneurons and a peripheral axon that terminates in the skin (Fig. 1B,C).

Adult animals possess many different types of somatosensory neurons, each specialized to sense distinct kinds of stimuli. Subtypes of sensory neurons can be distin-

guished molecularly by the expression of transcription factors that specify them, neurotrophin receptors that make them sensitive to specific growth factors, and ion channels that detect and transduce sensory stimuli (Lumpkin and Caterina, 2007; Marmigère and Ernfor, 2007). Morphologically, they can be distinguished by where their central axons project in the CNS, their association with glial cells (myelinating or unmyelinating), the distribution of vesicles and organelles that they contain (Kruger et al., 2003), and the morphology and localization of their peripheral terminals in the skin (Lumpkin and

Grant sponsors: National Research Service Award from the National Institute of Neurological Disorders and Stroke (to G.S.O.); National Institute of Dental and Craniofacial Research; Grant number: 5R01DE01849 (to A.S.).

Georgeann S. O'Brien's current address is Department of Molecular and Cell Biology, University of California, Berkeley, CA 94720.

\*CORRESPONDENCE TO: Alvaro Sagasti, Department of Molecular, Cell and Developmental Biology, University of California, Los Angeles, CA 90095. E-mail: sagasti@mcdcb.ucla.edu or JoAnn Buchanan, Department of Molecular and Cellular Physiology, Stanford University, Stanford, California 94305. E-mail: redhair@stanford.edu

Received June 17, 2011; Revised August 22, 2011; Accepted October 4, 2011

DOI 10.1002/cne.22791

Published online October 20, 2011 in Wiley Online Library (wileyonlinelibrary.com)

© 2011 Wiley Periodicals, Inc.

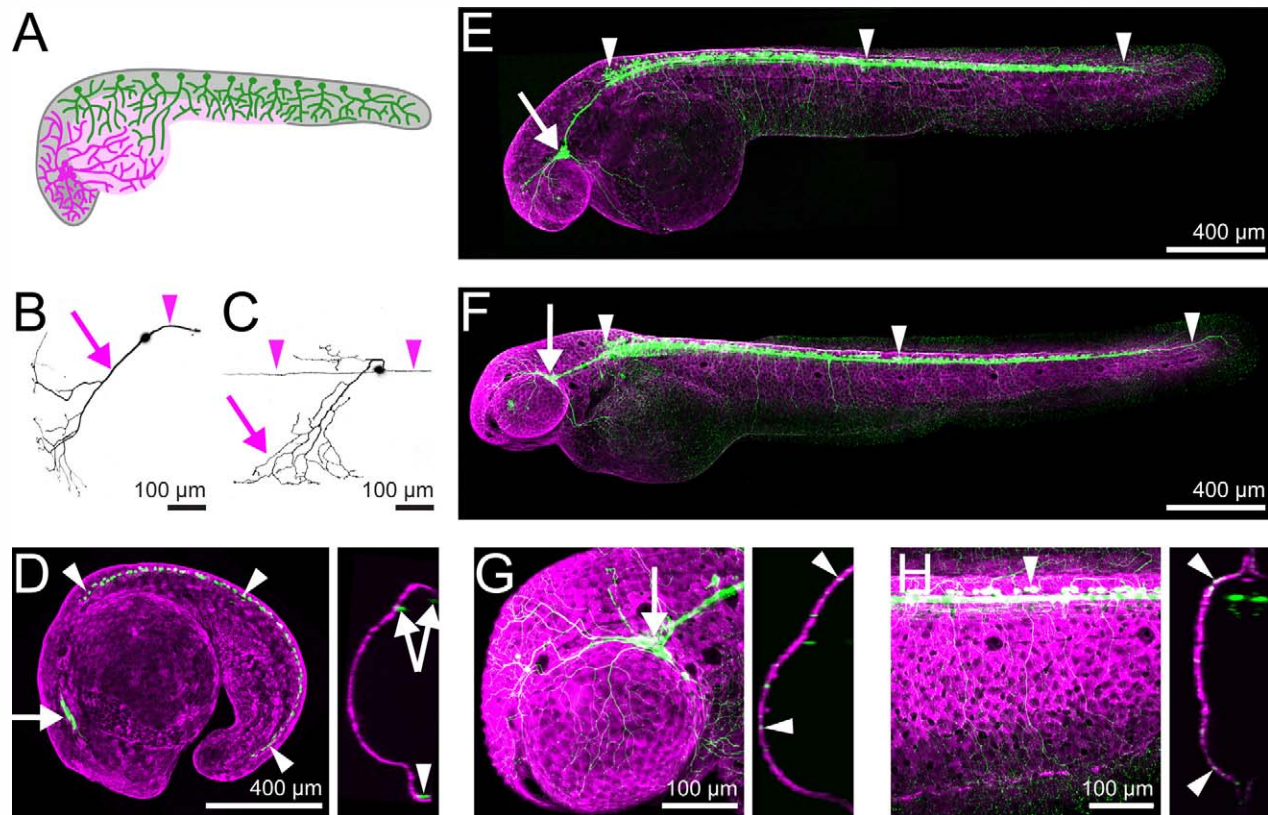


**Figure 1.** Live transgenic imaging allows visualization of peripheral sensory neurons and skin. **A:** Cartoon of ~30 hpf zebrafish showing locations of trigeminal (magenta) and RB (green) cell bodies and axons. **B,C:** Images of single 54-hpf trigeminal (B) and RB (C) neurons in transient transgenics reveal the structure of peripheral sensory neurons. Arrowheads indicate central axons and arrows indicate the peripheral axon that innervates the skin. **D-F:** Transgenic animals expressing sensory:GFP to highlight peripheral sensory neurons and keratin4:dsRED to highlight skin at 18 hpf (D), 36 hpf (E), and 54 hpf (F). Arrows point to trigeminal ganglia and arrowheads point to RB neurons. Image to the right of the 18 hpf embryo is an optical cross-section; note that the skin and neuronal staining do not overlap, indicating that it has yet to be innervated by sensory axons. **G,H:** Closeups of the trigeminal ganglion (G) and a region of the trunk above the yolk extension (H). Optical cross-sections to the right of each image reveal green sensory axons colocalizing with the skin (arrowheads). Scale bars = 100  $\mu\text{m}$  in B,C,G,H; 400  $\mu\text{m}$  in D-F.

Caterina, 2007). In adult vertebrates, including mammals and fish, mechanosensory peripheral axons are associated with a variety of specialized structures below the epidermis, such as Merkel cells, Pacinian corpuscles, hair follicles, and solitary chemosensory cells (Kotrschal et al., 1997; Kruger et al., 2003; Lumpkin and Caterina, 2007). Some peripheral axons are not associated with any particular structures; these axons emerge from myelin sheaths at the dermal/epidermal interface and branch extensively as “free endings” within the epidermis. Most of these free endings are thermosensory or nociceptive and have diverse morphologies and functions (Dubin and Patapoutian, 2010).

Peripheral sensory axons begin innervating the skin at early developmental stages, when it consists of just a few epithelial layers, suggesting that somatosensation is functional in embryos. For example, human DRG axons have reached the epidermis by 7 weeks of development (Moore and Munger, 1989), mouse trigeminal axons

begin innervating the skin at approximately E10.5 (Davies and Lumsden, 1984), and trigeminal and RB axons in zebrafish contact the skin between 16 and 18 hours post-fertilization (hpf) and become functional by 21 hpf (Kimmel and Westerfield, 1990; Saint-Amant and Drapeau, 1998; Sagasti et al., 2005). The ultrastructure of these earliest peripheral sensory axons is less well characterized than that of adult peripheral axons, and many questions about their development have yet to be completely answered. For example, how diverse are the morphologies of these earliest terminals? What is the structure of the skin at early stages of innervation? Does innervation by sensory terminals influence the maturation of the skin, as was suggested by a descriptive study of embryonic human skin (Moore and Munger, 1989)? Of particular interest to us is the nature of the association between sensory axons and skin cells: Where in the embryonic skin do peripheral axons arborize? Studies of RB innervation at early stages of *Xenopus* development found that RB

peripheral neurites form a plexus in the basal lamina, below the basal layer of keratinocytes (Roberts and Taylor, 1982; Taylor and Roberts, 1983). Endings of these axons pierce through small openings between basal skin cells (Taylor and Roberts, 1983), where they terminate between skin cells (Roberts and Hayes, 1977). In contrast, in the *Xenopus* head, two physiological distinct types of trigeminal mechanosensors project different types of terminals into the skin: type 1 neurites project branches between the skin layers and the lateral membranes of superficial cells; type 2 neurites branch both below and within the skin, but rarely between the superficial cells (Hayes and Roberts, 1983).

One intriguing possibility is that sensory axons in the skin course not only below or between skin cells but also within them, in much the same way that primary peripheral axons are sometimes enveloped by Schwann cells. Such associations between peripheral axons and skin cells have been described for adult fish and human skin (Cauna, 1973; Whitear and Moate, 1998) as well as for *Caenorhabditis elegans* (Chalfie and Sulston, 1981), but how common these structures are, whether they form in embryos, or what function they may serve have not been extensively explored.

## MATERIALS AND METHODS

### Animal care, transgenic zebrafish embryos, and morpholino injections

Zebrafish were maintained in 28.5°C, pH 7.5, water on a 14-hour/10-hour light/dark cycle. Animal care and experimental procedures were approved by the UCLA Chancellor's Animal Research Committee (ARC). ARC committee members and veterinary staff regularly inspected the zebrafish facility to ensure maintenance of animal care standards.

To image sensory neurons, we used the previously described Tg(sensory:GFP) and Tg(Isl2b:GFP) lines; to image keratinocytes, we created the Tg(keratin4:dsRED) line. Construction of the Tg(sensory:GFP) has been described by Sagasti et al. (2005). Briefly, this transgene includes a ~4.2-kb genomic EcoR1 fragment isolated from a BAC containing the islet1 gene (isl[ss]) by Higashijima et al. (2000). This genomic fragment is downstream of the islet1 gene and drives expression in a portion of the endogenous islet1 expression pattern. In the Tg(sensory:GFP) transgene, the isl[ss] region is used to drive expression of Gal4-VP16, which in turn binds to a stretch of 14 copies of the Gal4 UAS to drive expression of GFP. The use of Gal4-VP16 amplifies GFP expression, allowing GFP to fill comprehensively the entire axonal arbor, as evidenced by the fact that growth cone filopodia are clearly visible during development, arbors of dye-filled

axons expressing membrane-localized GFP are of comparable complexity (not shown), and the fact that anti-GFP and anti-alpha-tubulin staining colocalizes (see, e.g., Fig. 2C). The Tg(isl2b:GFP) line was created by Pittman et al. (2008). Briefly, this transgene uses a 17.6-kb fragment from directly upstream of the islet2b gene to drive expression of the GFP variant mmGFP5 in a variety of sensory neurons. To create Tg(keratin4:dsRED), we used a 2.2-kb enhancer region (amplified with the primers 5'-GAATTCCTACAGTAAAGCTTCTCCACAATGTCCC-3' and 5'-GGATCCCTCTGCGTGTCTCTCAGCAGCTGGCTG-3') from directly upstream of the keratin 4 gene (previously known as keratin 8; Gong et al., 2002) to drive expression of dsRED directly. All of these transgenes segregate in a straightforward Mendelian fashion, indicating that they have integrated at a single genomic locus, although that locus has not been mapped. Observations of transgenic embryos were made in dozens of individual embryos from several clutches obtained on different days.

To prevent the development of peripheral sensory neurons, embryos were injected with 3–5 nl of 0.7 mM *neurogenin-1* (*ngn-1*) morpholino (5'-ACGATCTCCATTGTTGATAACCTGG-3'; Andermann et al., 2002; Cornell and Eisen, 2002) at the one-cell stage. Loss of sensory neuron expression in the Tg(Isl2b:GFP) line was monitored to confirm the efficacy of the morpholino.

### Confocal imaging

Live zebrafish embryos were mounted for imaging by anesthetizing them in 0.02% tricaine and were immobilized in 1% low melt agarose. Mounted embryos were imaged with a Zeiss LSM 510 confocal microscope as previously described (O'Brien et al., 2009).

### Antibody characterization

To visualize basement membranes, we used a rabbit polyclonal antibody against laminin purified from the basement membrane of a mouse sarcoma (Table 1), which has previously been used in zebrafish (Costa et al., 2008). We recapitulated an expression pattern similar to that previously reported. Specifically, this antibody stained basement membranes (a thin, continuous band below epithelia) throughout the embryo. To verify the specificity of this antibody further, we stained embryos injected with 4.5 ng of a morpholino (5'-TGTGCCTTTTGCTATTGCGACCTC-3') targeting the laminin c1 (*lamc1*) gene (Parsons et al., 2002). In severely affected embryos injected with this morpholino (as judged by having a severely shortened body axis), antilaminin staining in basement membranes was absent, and, in mildly affected embryos (less severely shortened body axis), it was reduced or patchy (not shown).

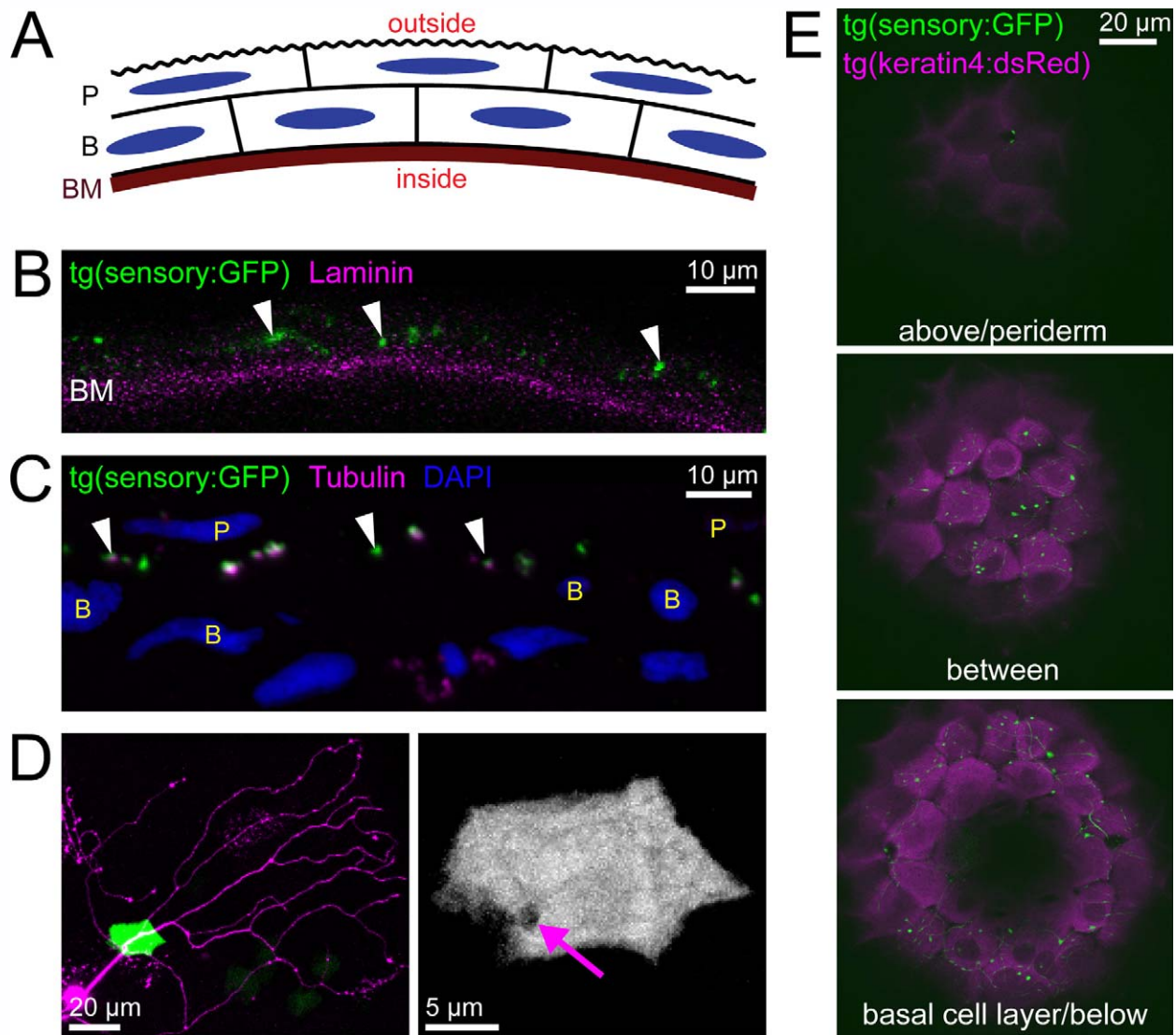


**Figure 2.** Peripheral sensory axons arborize within the skin. **A:** Diagram of the embryonic zebrafish skin. The skin consists of two layers, the periderm (P) and basal cell layer (B). The basement membrane (BM) is located below the basal cell layer. **B:** Antibody stain for GFP (green) and laminin (magenta) in a vibratome section of a *tg(sensory:GFP)* fish at 54 hpf. GFP-expressing peripheral axons (arrowheads) localized exterior to the band of laminin staining. **C:** Antibody stain for GFP (green) and tubulin (magenta) in a 70-nm microtome section of a 78 hpf *sensory:GFP* transgenic fish. Cell nuclei labeled with DAPI (blue; P, periderm nucleus; B, basal cell nucleus). Peripheral sensory axons (arrowheads) are exclusively located between the nuclei of the two epidermal cell layers. **D:** By using transient transgenesis to achieve mosaic expression of both transgenes, a single sensory axon (magenta) was imaged extending its primary axon through a skin cell (green) and arborizing above it. Maximum projection of a confocal image stack taken of the head of a live embryo at 54 hpf. Right, green channel only, showing an opening in the skin cell through which the axon enters (arrow). **E:** Three confocal optical sections showing a dorsal view of the top of the head of an embryo harboring the *sensory:GFP* and *keratin4:dsRED* transgenes. All labeled axons arborized between the two skin layers. In the top panel, two green dots are visible, which appear to be axonal varicosities that bulge up into the optical plane of the outer layer of skin cells. Scale bars = 10  $\mu$ m in B,C; 20  $\mu$ m in D (left), 5  $\mu$ m in D (right).

To visualize axons, we used a mouse monoclonal antiacetylated  $\alpha$ -tubulin antibody (Table 1) that has been used in zebrafish to visualize axons (Olsson et al., 2008). We recapitulated an expression pattern similar to that previously reported for tubulin staining. As expected for an axonal marker, tubulin staining was visible in the stereotyped pattern of the major axon tracts of the zebrafish embryo as well as the fine arbors of peripheral axons in the skin. Array to-

mography further verified the specificity of this antibody by confirming that tubulin staining colocalized with staining for GFP in *Tg(sensory:GFP)* embryos (see Fig. 2C).

### Antibody staining

Embryos were fixed in 4% paraformaldehyde for 10 minutes at room temperature, then overnight at 4°C, followed by permeabilization in acetone for 8 minutes at

**TABLE 1.**  
Primary Antibodies

Antigen	Immunogen	Antibody details	Dilution used
Laminin	Laminin purified from basement membrane of EHS mouse sarcoma	Sigma; rabbit polyclonal; No. L9393	1:100
Acetylated alpha-tubulin	Acetylated alpha-tubulin from the outer arm of sea urchin sperm axonemes	Sigma; mouse monoclonal; No. T6793	1:200
GFP (for costaining with antilaminin)	GFP isolated from <i>Aequorea victoria</i>	Invitrogen (Molecular Probes); mouse monoclonal; No. A11120	1:500
GFP (for costaining with antitubulin)	GFP isolated from <i>Aequorea victoria</i>	Invitrogen; rabbit polyclonal; No. A11122	1:100

–20°C and whole mount antibody staining. Embryos were incubated in primary antibodies rabbit  $\alpha$ -laminin (1:100) and mouse  $\alpha$ -GFP (1:500) overnight at 4°C (Table 1). On the following day, embryos were incubated in secondary antibodies Cy5  $\alpha$ -rabbit (1:500) and Cy2  $\alpha$ -mouse (1:200) for 4 hours at room temperature. Embryos were embedded in agarose and cut into 200- $\mu$ m sections with a vibratome, mounted on coverslips, and imaged with a Zeiss LSM 510 confocal microscope. At least 10 embryos were stained and imaged for this experiment.

### Array tomography

For antibody staining of ultrathin sections (see Fig. 2C), fixed embryos were embedded in LR white resin, cut on a Reichert ultramicrotome into a ribbon of 70-nm sections, and mounted on a coverslip (Micheva et al., 2010). Sections were stained with mouse antitubulin (1:200) and rabbit anti-GFP primary antibodies (1:100; Table 1), followed by Alexa 594 anti-mouse and Alexa 488 anti-rabbit secondary antibodies (1:50). See Micheva et al. (2010) for details on sectioning and staining protocol. After staining, sections were treated with ProLong Antifade with DAPI (Invitrogen, Carlsbad, CA) and imaged using a Zeiss Axio Imager with a  $\times 63$  oil objective. At least 10 embryos were stained and imaged for this experiment.

### Transmission electron microscopy

Embryos were anesthetized for 10 minutes in 0.02% tricaine before fixation in 4% paraformaldehyde, 2% glutaraldehyde in 1 $\times$  PBS (pH 7.4); placed on a rotator for 2 hours at room temperature; and incubated at 4°C overnight. Fixed embryos were washed for 3  $\times$  10 minutes with PBS, treated with 1% osmium for 1 hour, and washed for 3  $\times$  5 minutes with ddH<sub>2</sub>O. Embryos were then dehydrated with an ethanol series, switched into propylene oxide (PO) for 2  $\times$  10 minutes, and infiltrated with epoxy resin through a series of steps (1:1 PO:epoxy for 30 minutes, 1:2 PO:epoxy for 2 hours, 100% epoxy overnight). On the next day, embryos were transferred into coffin molds with freshly made epoxy resin and oriented head first. Molds were maintained under vacuum (12 in.

Hg) for  $\geq 2$  hours to remove air bubbles and were hardened at 60°C for 48 hours. Blocks were trimmed into a trapezoid shape with a Leica EM trimmer. Ultrathin 70-nm sections were cut on a Reichert Ultracut microtome using a diamond knife. Sections were collected on formvar-coated slot grids (two to four sections per grid) and allowed to dry, as described by Harris et al. (2006) and poststained using uranyl acetate and lead citrate. Imaging was done on several TEM microscopes, including a Zeiss 10CA (Marine Biological Laboratory, Woods Hole, MA), a JEOL 100CX (UC Berkeley, Berkeley, CA), and an FEI Technai (UCLA, Los Angeles, CA). At least two embryos were examined by TEM analysis at each time point.

### Serial scanning electron microscopy

Conventionally prepared resin blocks were cut with a jumbo Histo diamond knife (Diatome; EMS, Fort Washington, PA). Ribbons of ultrathin 70-nm sections were collected on carbon-coated glass coverslips and allowed to dry. Sections were stained with a copper/lead solution directly on the coverslips for 30 minutes in a closed plastic petri dish containing NaOH pellets (Thiéry et al., 1995). Ribbons were washed three times with filtered ddH<sub>2</sub>O and allowed to dry overnight in a dust-free environment. Coverslips were attached to the stage using conductive copper tape (Ted Pella, Redding, CA). Serial sections were imaged with a Zeiss Gemini Sigma SEM at 7 kV using a 60- $\mu$ m aperture in the backscatter mode. Images were recorded using a scan speed of 8–10 and dwell time of 1  $\mu$ sec/pixel. Pixel size ranged from 3 to 100 nm per pixel. Images were reconstructed in Reconstruct (<http://synapses.clm.utexas.edu/tools/reconstruct/reconstruct.stm>). Series of adjacent sections were collected in six different regions from the heads of three animals. Three of these were reconstructed and are shown in Figure 8.

## RESULTS

### Zebrafish peripheral sensory axons initially arborize between two epithelial layers

To investigate how the peripheral axons of the earliest-born vertebrate somatosensory neurons establish their

cutaneous territories, we imaged zebrafish peripheral axons with a stable reporter line harboring a transgene that drives GFP expression specifically in trigeminal and RB neurons (sensory:GFP; Fig. 1; Sagasti et al., 2005). At embryonic and early larval stages, the zebrafish skin consists of two epithelial cell layers, the outer periderm and inner basal cell layer; the basal cell layer is separated from underlying tissues by a laminin-rich basement membrane (Fig. 2A; Le Guellec et al., 2004). To assess sensory axon localization relative to the basement membrane in zebrafish, we first stained 54 hpf sensory:GFP transgenic embryos with antilaminin and anti-GFP antibodies, generated vibratome cross-sections, and imaged them via confocal microscopy. Confocal imaging of GFP-labeled trigeminal sensory axons showed that they were always located outside of the laminin layer (Fig. 2B), except close to the cell bodies from which primary axons project. Similarly, array tomography (AR) of sensory:GFP embryos with anti-GFP, antitubulin, and DAPI, suggested that sensory axons are located between the two outermost cell layers of the embryo (Fig. 2C). These observations indicated that sensory axons arborize within the skin, rather than within the basement membrane.

To determine more precisely where peripheral axons arborize within the skin, we created a transgenic line in which dsRED expression is driven exclusively in skin cells (keratin4:dsRED), crossed this line to sensory:GFP, and imaged live animals via confocal microscopy between 18 and 78 hpf (Fig. 1D–H). Consistently with antibody staining results, primary branches of both trigeminal and RB peripheral axons projected directly to the skin, penetrated the basal cell layer, and branched between the two layers of skin (Fig. 2D,E). The primary branch of each trigeminal peripheral axon extended from the soma for an average distance of 84  $\mu\text{m}$  before entering the skin (range 38–140  $\mu\text{m}$ ). Most primary branches of trigeminal neurons extended as individual axons, except for one group of axons that appeared to form a bundle over the eye before branching in the rostral portion of the head, which may be analogous to the ophthalmic branch of the trigeminal in other organisms. RB peripheral axons extended as solitary axons dorsolaterally away from the spinal cord for an average of 26.65  $\mu\text{m}$  (range 13–35  $\mu\text{m}$ ) before entering the skin.

Once between the two skin layers, peripheral axons of trigeminal and RB neurons branched extensively (Figs. 1, 2D,E). Because they were sandwiched between the two epithelial layers, arbors were confined to a two-dimensional plane. The primary axon extended from the cell body to the skin, but GFP-expressing axons and dsRED-expressing skin cells colocalized throughout the branched portion of the arbor (Fig. 1G,H). Often, the primary branch abruptly changed trajectory at the point

where it entered the skin. We imaged isolated skin cells and axons using transient transgenesis to visualize more clearly the area where axons penetrated the skin. In some instances, axons appeared to have distorted the edge of a basal cell to create an omega-shaped channel through which the axon entered the skin (Fig. 2D).

To characterize the ultrastructure of skin and peripheral sensory axons at early stages, zebrafish embryos were fixed at 54 hpf and prepared for TEM. Neurite-like profiles were detected between skin cell layers in the head but were detected neither below the skin nor between the lateral membranes of skin cells, as predicted from confocal microscopy (asterisks in Fig. 3A and Fig. 4E–F). These profiles had many of the hallmarks of axons, including the presence of mitochondria, microtubules (best seen in a longitudinal slice, e.g., Fig. 7C), and polyribosomes (e.g., Fig. 6C). The diameter of these neurite-like profiles ranged from approximately 0.1 to 2  $\mu\text{m}$ , suggesting that individual axons may vary substantially in diameter. To determine whether trigeminal and RB neurons display similar arborization patterns, we performed TEM analysis on the trunk and tail fin at similar stages (Fig. 5). As in the head, similar neurite-like profiles were located between the two epithelial layers throughout the body.

To test whether these neurite-like structures were somatosensory peripheral axons, embryos were injected with *neurogenin-1* morpholino antisense oligonucleotide (*ngn-1* MO) at the one-cell stage, which prevents the development of peripheral sensory neurons (Andermann et al., 2002; Cornell and Eisen, 2002), and fixed at 54 and 78 hpf for TEM. No neurite-like profiles were observed between skin cells in these *ngn-1* morphants. In the absence of sensory axons, the membranes of peridermal cells and basal keratinocytes were closely apposed and held together by many cell junctions (Fig. 3B,D). To verify further the identity of the neurite-like profiles, embryos were fixed 1.5 hours after two-photon ablation of an entire trigeminal ganglion, which caused rapid fragmentation and degeneration of all the axons innervating half the head (O'Brien et al., 2009; Martin et al., 2010). In TEM images of these ablated animals, swollen and fragmented membranes appeared in place of the neurite-like profiles typically seen in uninjured embryos (Fig. 3E,F). Together, these observations demonstrate that, at early stages of innervation, the peripheral sensory axons of all somatosensory neurons in zebrafish arborize exclusively between the two epithelial layers that make up the larval skin.

### Skin cells mature as sensory axons arborize

Peripheral axons begin extending from trigeminal and RB neurons between 16 and 18 hpf (Kimmel and Westerfield, 1990). To characterize the time course of skin and peripheral sensory axon development, zebrafish embryos

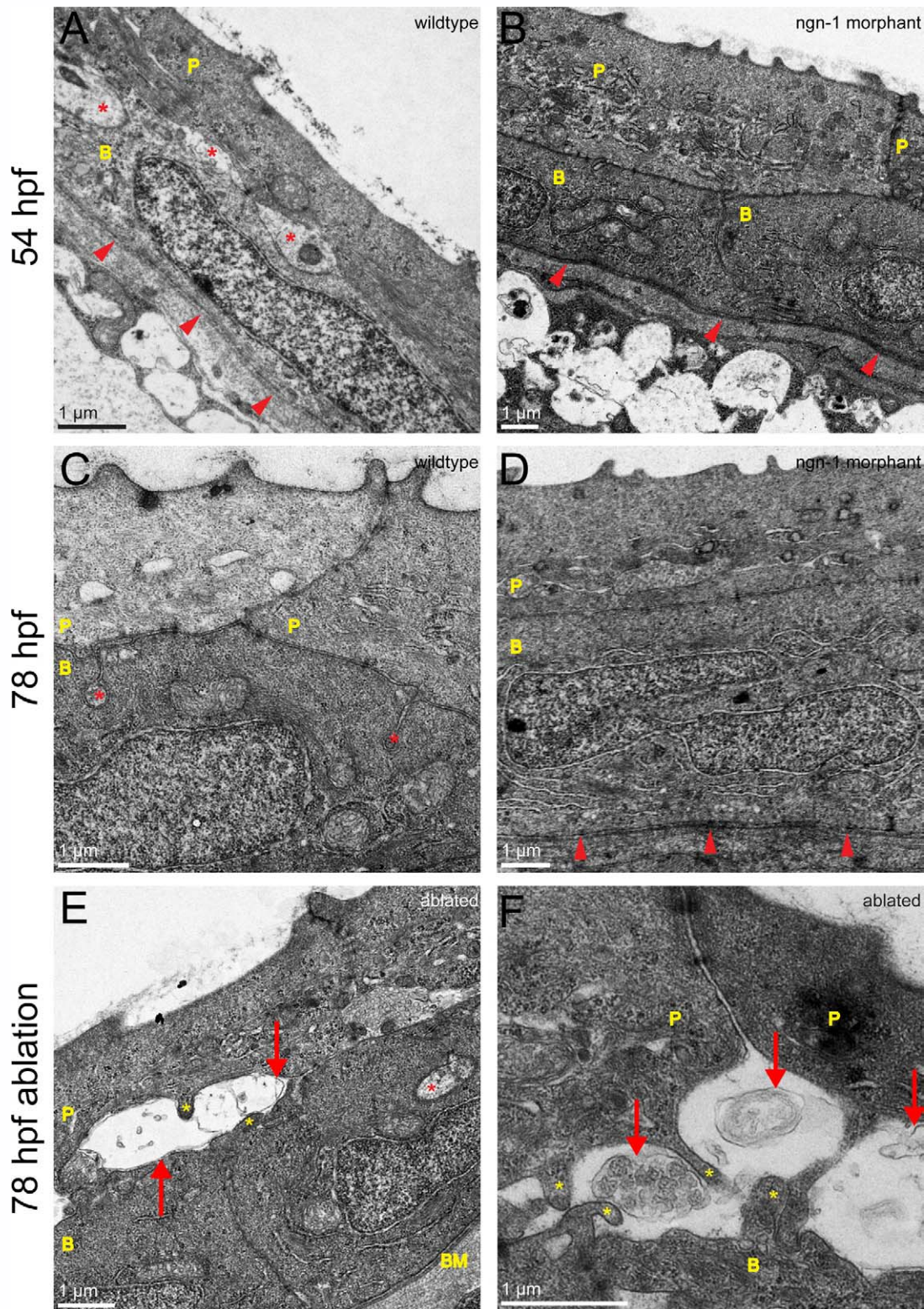


**Figure 3.** Putative neurite profiles in the wild-type zebrafish skin are absent in *neurogenin-1* morphants and degenerate after sensory neuron ablation. A–D: TEM images of the zebrafish epidermis at 54 hpf (A,B) and 78 hpf (C,D). P, peridermal cell; B, basal cell; arrowheads point to basement membrane. Orientation for all EM images is periderm upward. A,C: Wild-type embryos at 54 (A) and 78 (C) hpf. Asterisks indicate neurite-like profiles. B,D: *neurogenin-1* Morphant embryos at 54 (B) and 78 (D) hpf. No neurite-like profiles were observed. E,F: TEM images of the zebrafish epidermis at 79.5 hpf. All the cell bodies of one trigeminal ganglion were laser ablated at 78 hpf. Images were acquired  $\geq 200 \mu\text{m}$  from the site of ablation. Red arrows point to degenerating axon membranes and organelles. Yellow asterisks indicate skin cell protrusions toward the degenerating axon. The red asterisk in E indicates a seemingly intact axon. Such degenerating axon profiles were not seen on the contralateral side of the head, where trigeminal innervation remained intact. Scale bars = 1  $\mu\text{m}$ .

were fixed at 18, 24, 30, 54, and 78 hpf and imaged via TEM. At 18 hpf, when peripheral sensory axons are first extending, peridermal cells and basal keratinocytes were present, but the basal cell layer appeared relatively immature (Fig. 4A,B). There was no discernible basement membrane below basal cells. The periderm had microridges along its outer edge and apical tight junctions connected peridermal cells to one another (arrowhead in Fig. 4B), but no electron-dense junctions connected periderm to basal cells or basal cells to one another. Putative neurite-like profiles that could be the primary branches of growing peripheral sensory axons were found below the basal cell layer (asterisks in Fig. 4A,B) but not between epidermal cell layers.

By 30 hpf, neurite-like profiles were detectable between the two skin layers (arrows in Fig. 4C,D) and were often surrounded by large pockets of extracellular matrix (ECM). A faintly electron-dense, discontinuous basement membrane was present beneath the basal cell layer, and desmosomes or adherens junctions connected basal cells to one another as well as to overlying peridermal cells (e.g., red arrowhead Fig. 4C). At 54 hpf, many more junctions were visible between skin cells (red arrowheads in Fig. 4E), and the basement membrane formed a continuous and clearly defined, electron-dense band running beneath the basal cell layer. More neurite-like profiles were observed between skin cell layers at this stage (asterisks in Fig. 4E,F), often containing mitochondria (m in Fig. 4F). Most of the ECM surrounding axons at early stages had disappeared, and axon membranes were closely apposed to neighboring skin cell membranes (arrow in Fig. 4F).

### Basal keratinocytes envelop peripheral sensory axons

In addition to the axon profiles between skin cell layers at 54 hpf, we sometimes observed neurite-like profiles enveloped within basal skin cells (double arrowhead in Fig. 4E). At 78 hpf, these enveloped neurite-like structures were more common (Figs. 6–8) and were also sometimes found between the lateral membranes of two basal cells. To verify the identity of these structures, we again examined *ngn-1* morphants via TEM. As expected, these enveloped neurite-like structures were largely absent in *ngn-1* morphants (Fig. 3C,D). We further confirmed the identity of these profiles by laser ablating trigeminal neuron cell bodies at 78 hpf and imaging the heads of these larvae via TEM 1.5 hours after ablation. The neurite-like structures between and within skin cells exhibited signs of degeneration in these ablated animals, confirming that they were peripheral sensory axons (Fig. 3E,F).

Enveloped axons were tightly surrounded by basal skin cell membrane, which invaginated to form convoluted channels in the basal cell, with enveloped axons contained at the bottom of these channels (Fig. 6). These channels

were usually sealed with desmosomes or adherens junctions, securing the enveloped axon in a tight pocket (e.g., Figs. 6B,C, 7A). In some cases, enveloped axons sectioned along their longitudinal axis were observed to extend lengthwise through the basal cell (Figs. 6D, 7C).

In addition to TEM analysis, we also imaged serial sections of 78 hpf larvae by SEM. Because of the different post stains used, SEM analysis revealed different features of sensory axon innervation. For example, although in TEM images the membranes of enveloped axons seemed to abut directly the membrane of the basal keratinocyte, in SEM images an electron-dense material, similar in appearance to the basement membrane below the basal cells, was often visible, apparently between the two membranes (Fig. 7). This may suggest that a specialized ECM, perhaps akin to the “mantle” that surrounds mechanosensory neurons in *C. elegans* (Goodman, 2006), surrounds enveloped zebrafish peripheral sensory axons.

### Sensory axons project through long tunnels within basal skin cells

To describe the 3-D ultrastructure of enveloped sensory axon branches, we reconstructed serial sections of scanning electron micrographs in three-dimensions using Reconstruct software (Harris et al., 2006). The durability of serial sections on coverslips for serial scanning electron microscopy (sSEM) makes them much easier to use than TEM sections for reconstructing 3-D structures from many adjacent sections. Using sSEM analysis, we were able to follow axons through significant portions of their trajectories and created 3-D reconstructions of several micrometers in three different areas of the head (Fig. 8). Reconstructed axons often tunneled for at least several micrometers within furrows in basal keratinocytes, and individual enveloped axons coursed from one basal cell to another (Fig. 8E). In some cases axons were partially enveloped by a basal cell and partially between the two epithelial layers (purple axon in Fig. 8E). Skin cell membranes formed a convoluted channel that sealed the axon away from the outside environment (e.g., Fig. 8H). In 3-D reconstructions, the diameter of individual axons varied extensively (from 0.1 to 2  $\mu\text{m}$ ). Large varicosities filled with mitochondria were occasionally seen (Fig. 8A–C), corresponding to the larger axon diameter profiles that we had noted in TEM sections, and an electron-dense material was often found at the terminal tip of axon branches.

## DISCUSSION

### Peripheral axons initially arborize between two epithelial layers

We have described the first wave of somatosensory peripheral axon endings to innervate the skin of the head, trunk, and tail fin in zebrafish, using live transgenic imaging

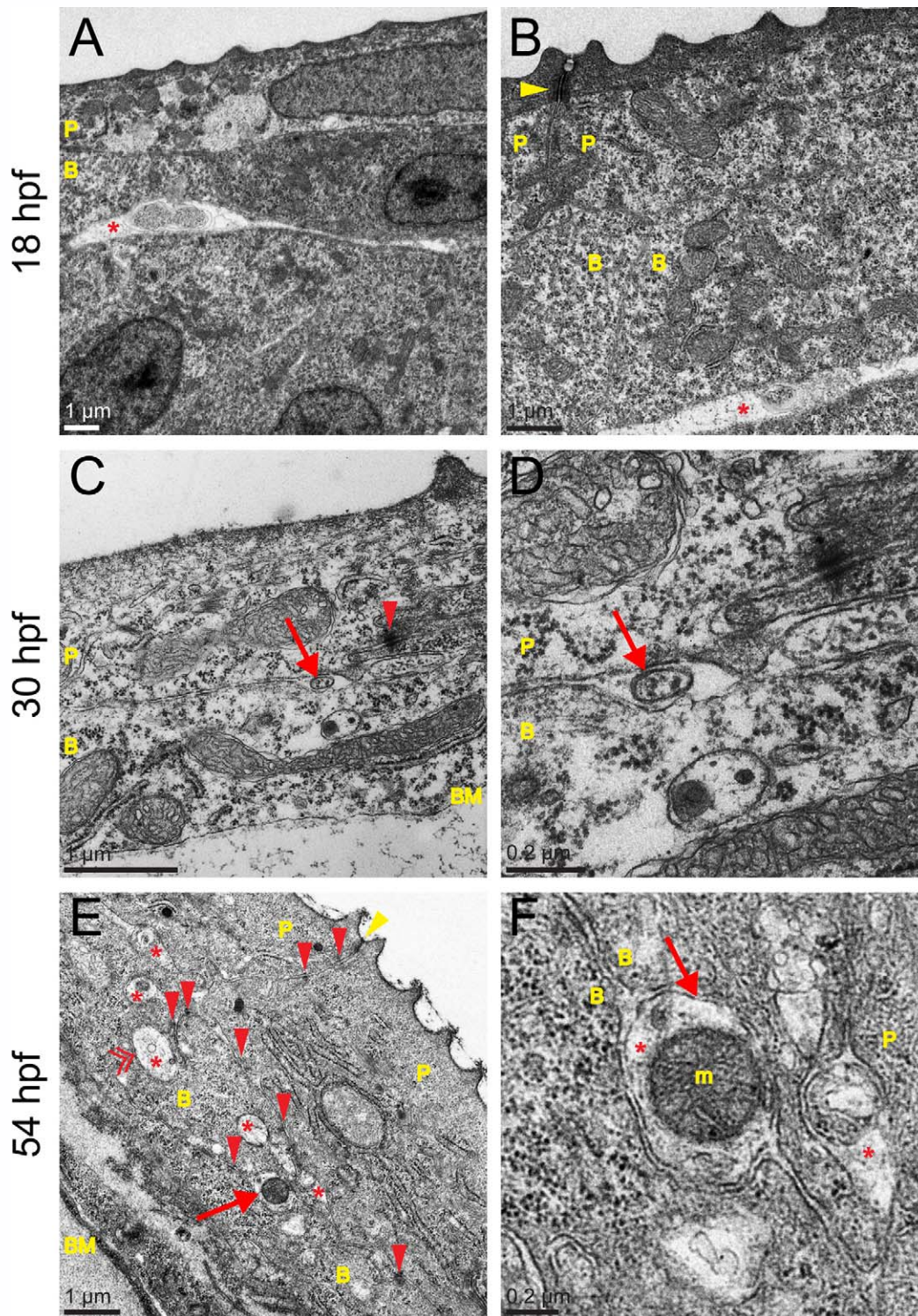


**Figure 4.** Ultrastructure of zebrafish skin and trigeminal sensory axons at several development stages. TEM images of the wild-type zebrafish epidermis at 18, 30, and 54 hpf. P, peridermal cell; B, basal cell; BM, basement membrane; m, mitochondrion. **A,B:** The skin consisted of two layers at 18 hpf. Although tight junctions joined the apical ends of peridermal cells (arrowhead), no adherens junctions or desmosomes appeared to hold skin cells together. Asterisks indicate potential neurite profiles located below the immature basal cell layer. **C,D:** At 30 hpf, adherens junctions or desmosomes appeared at relatively low frequency between skin cells (red arrowhead); an immature basement membrane (BM) was present. The arrow in C indicates the axon shown at higher magnification in D. **E:** At 54 hpf, many more cell junctions were present (red arrowheads), and an electron-dense, continuous BM was apparent. Yellow arrowhead indicates an apical tight junction. Asterisks indicate the many axons observed in the skin by this time. Arrow indicates the axon shown at higher magnification in F. Double arrowhead indicates an axon enveloped within a basal cell. **F:** Two axons are visible (asterisks), one containing a large mitochondrion and clearly defined axon membrane (arrow) distinct from the two basal cell membranes that surround it. Scale bars = 1  $\mu\text{m}$  in A-C,E; 0.2  $\mu\text{m}$  in D,F.

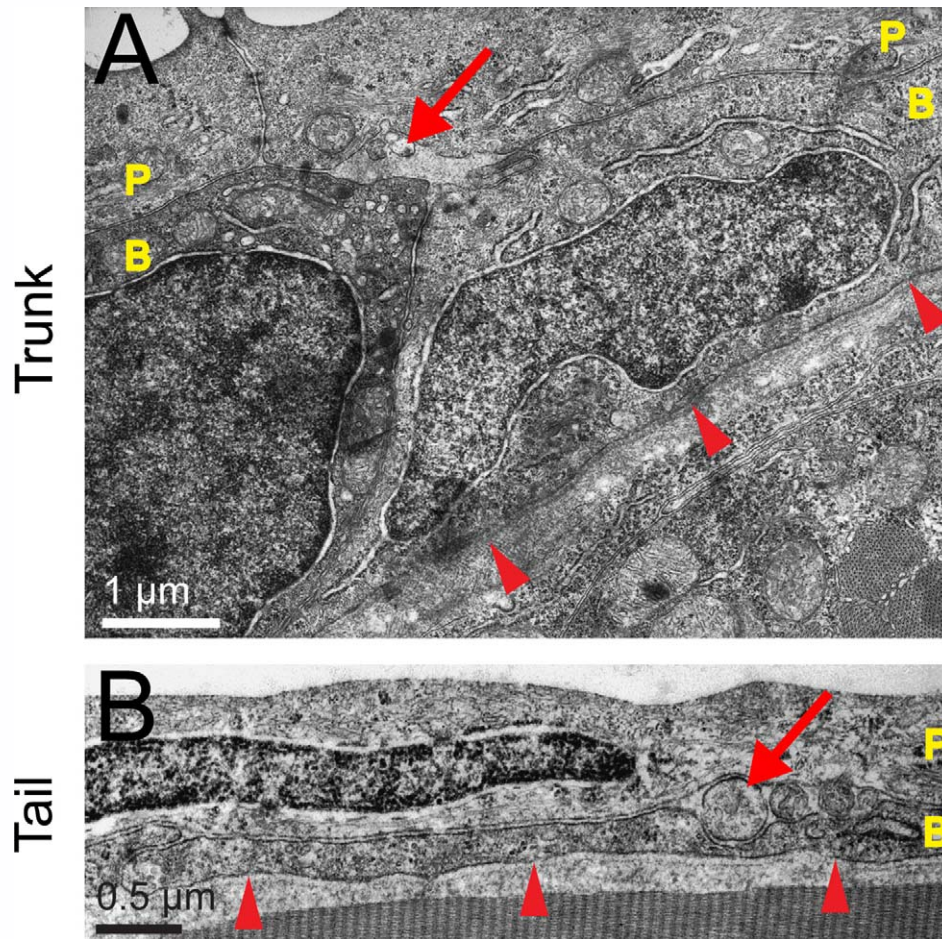


**Figure 5.** Innervation of the zebrafish skin in the trunk and tail. TEM images of the wild-type zebrafish epidermis in the trunk at 48 hpf (A) and the tail fin at 72 hpf (B). P, peridermal cell; B, basal cell; arrowheads indicate basement membrane; arrows point to axon profiles between the periderm and basal cell layers. Scale bars = 1 µm in A; 0.5 µm in B.

and electron microscopy. The innervation patterns that we describe are likely to be conserved among teleost fish and, in at least some features, among all vertebrates. Similar neurite profiles of free nerve endings have been described for the epidermis of adult minnow, stickleback, sand goby, and sapphirine gurnard fish (Whitear, 1971) as well as in developing *Xenopus* and human skin (see, e.g., Cauna, 1973; Breathnach, 1977; Roberts and Hayes, 1977; Hayes and Roberts, 1983; Kennedy and Wendelschafer-Crabb, 1993).

When zebrafish peripheral sensory axons first reach the periphery, the skin consists of two epithelial layers: the outer periderm, which derives from the early embryonic enveloping layer, and the inner layer of basal keratinocytes, which derives from the ectodermal lineage (Le Guellec et al., 2004). Confocal imaging of transgenic zebrafish embryos revealed that the primary axons of trigeminal and RB neurons projected directly to the skin and infiltrated between basal cells to reach the region between the two cell layers. Most, if not all, axon branching occurred in the territory between the two skin layers.

The small conduits that we observed in the basal cell layers through which axons traversed likely were created by the axons (rather than pre-existing in the skin), because we never saw an unoccupied conduit.

Early somatosensory innervation of vertebrate skin has been most comprehensively described for *Xenopus* embryos (Roberts and Blight, 1975; Roberts and Hayes, 1977; Roberts and Taylor, 1982; Davies et al., 1982; Hayes and Roberts, 1983; Kitson and Roberts, 1983; Taylor and Roberts, 1983). These studies showed that the peripheral neurites of somatosensory neurons also reached the skin when it consisted of two epithelial layers. Two distinct classes of trigeminal neurons in *Xenopus* displayed different innervation patterns: “type 1” neurites arborized entirely within the skin and often between superficial skin cells, whereas “type 2” neurites arborized both below and within the skin but only rarely within the superficial layers (Roberts and Hayes, 1977; Hayes and Roberts, 1983). RB neurons in *Xenopus* form an elaborate plexus beneath the skin and project branches that terminate between skin cells (Roberts

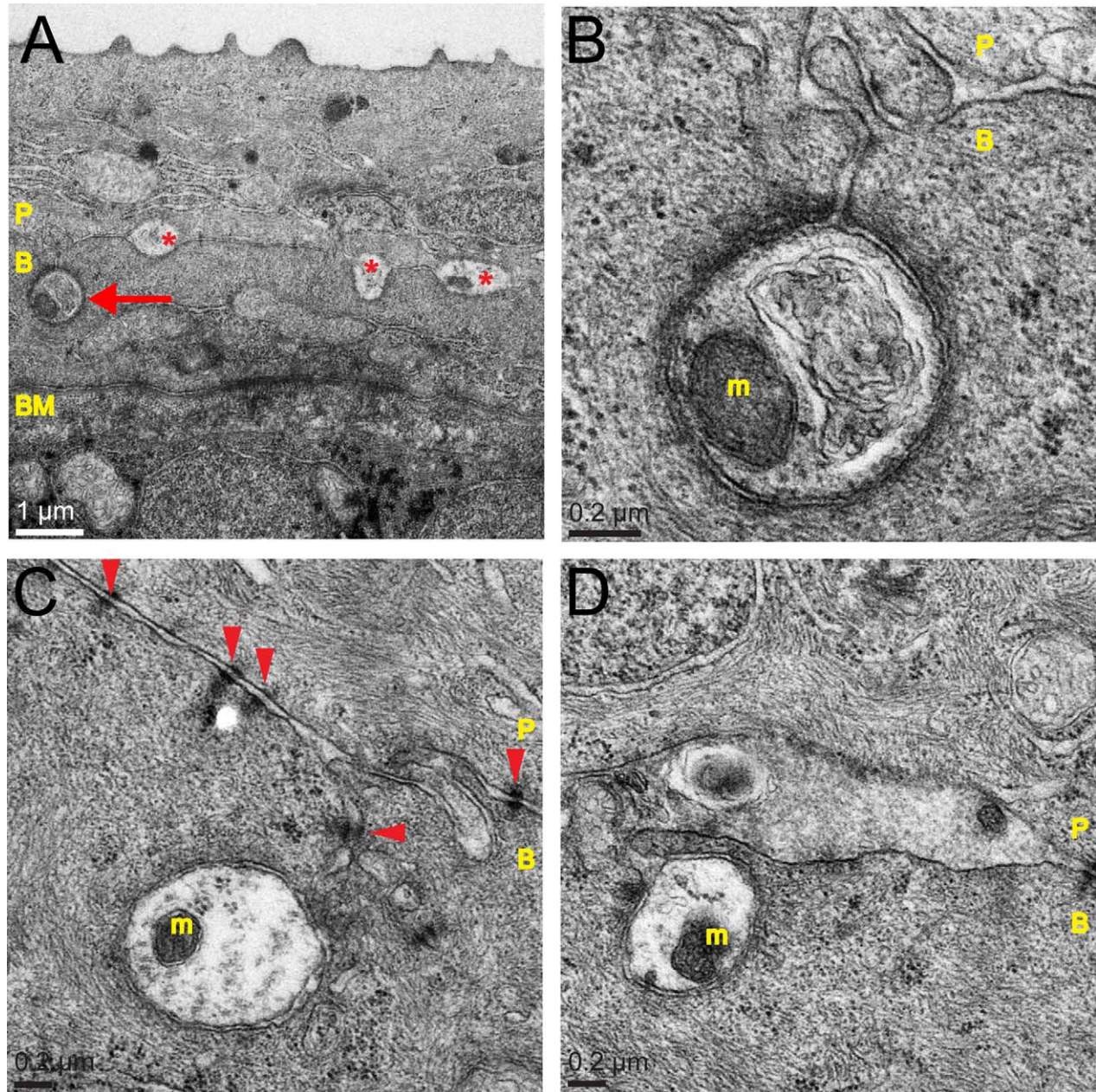


**Figure 6.** Basal skin cells frequently envelop axons at 78 hpf. TEM images of the wild-type zebrafish epidermis at 78 hpf. P, peridermal cell; B, basal cell; BM, basement membrane; m, mitochondrion. **A:** Axons were found between epidermal cells (asterisks) and enveloped within basal cells (arrow). **B:** Higher magnification of axon indicated by arrow in A. **C:** An enveloped axon. Many cell junctions join the skin cell membranes (arrowheads). **D:** Possibly two branches of the same axon, one in cross-section and the other in longitudinal section. Note that in axons in B–D a clearly defined axon membrane appears to be in contact with, but is distinct from, the epidermal cell membranes surrounding it. Scale bars = 1  $\mu\text{m}$  in A; 0.2  $\mu\text{m}$  in B–D.

and Hayes, 1977; Roberts and Taylor, 1982; Taylor and Roberts, 1983). Unlike type 1 trigeminal neurons in *Xenopus*, zebrafish trigeminal neurons were never located between superficial skin cells, and, unlike type 2 trigeminal neurons or RB neurons in *Xenopus*, they never arborized below the skin. Our study has thus revealed both similarities and differences between the innervation strategies of somatosensory peripheral axons in fish and amphibians. Whether these

structural differences reflect functional differences in somatosensory neuron subtypes awaits a definitive physiological study of early trigeminal and RB neurons in zebrafish.

### Peripheral sensory axons and skin develop together

We found that all zebrafish peripheral sensory axons in the first wave of innervation were free endings and that

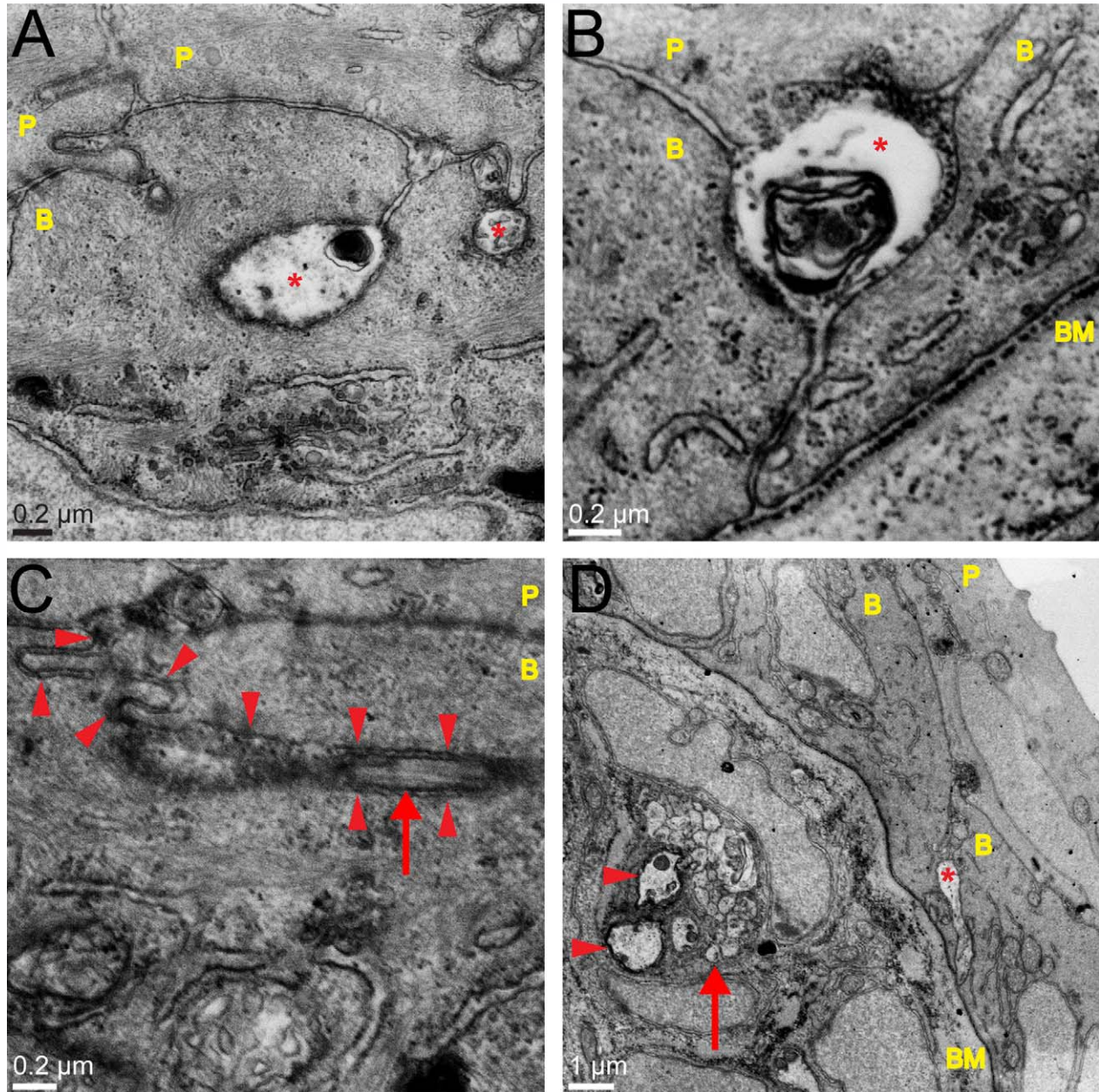


**Figure 7.** SEM reveals that axons are enveloped by basal cells and surrounded by an electron-dense material at 78 hpf. SEM images of the wild-type zebrafish epidermis at 78 hpf. P, peridermal cell; B, basal cell; BM, basement membrane; asterisks indicate axons. **A:** An axon enveloped within a basal skin cell, with an electron-dense substance surrounding the axon membrane. **B:** An axon located between two basal cells, with an electron-dense substance between the axon and skin cell membranes. **C:** Arrow points to a longitudinal section of an axon. Note the microtubules, distinct axon membrane, and envelopment by basal cell membranes (arrowheads). **D:** An axon bundle (arrow) located beneath the skin, just dorsal to the eye; this may be a mix of trigeminal and lateral line sensory axons. Two of the axons are myelinated (arrowheads). Asterisk indicates a putative axon shown in longitudinal section, extending through the BM into the epidermis. Scale bars = 0.2  $\mu\text{m}$  in A–C; 1  $\mu\text{m}$  in D.

all skin cells at these stages were unspecialized epithelial cells. Even at these early stages, zebrafish respond to diverse mechanosensory, chemical, and thermal somatosensory stimuli (Saint-Amant and Drapeau, 1998; Prober et al., 2008), suggesting either that these neurons are polymodal or that there are several distinct sensory neuron

types with similar morphologies. In *Xenopus*, for example, the head is innervated by at least two physiologically distinct types of trigeminal neurons with similar morphologies (Roberts, 1980). Several genes are expressed in subsets of zebrafish trigeminal and RB neurons at these stages (Martin et al., 1995, 1998; Slatter et al., 2005;

Kucenas et al., 2006), favoring the conclusion that, despite their uniform ultrastructure, there are at least a few types of distinct sensory neuron subclasses.

Our analyses revealed that innervation of the skin coincided with the maturation of the basal keratinocyte layer. At 18 hpf, when trigeminal and RB peripheral axons first

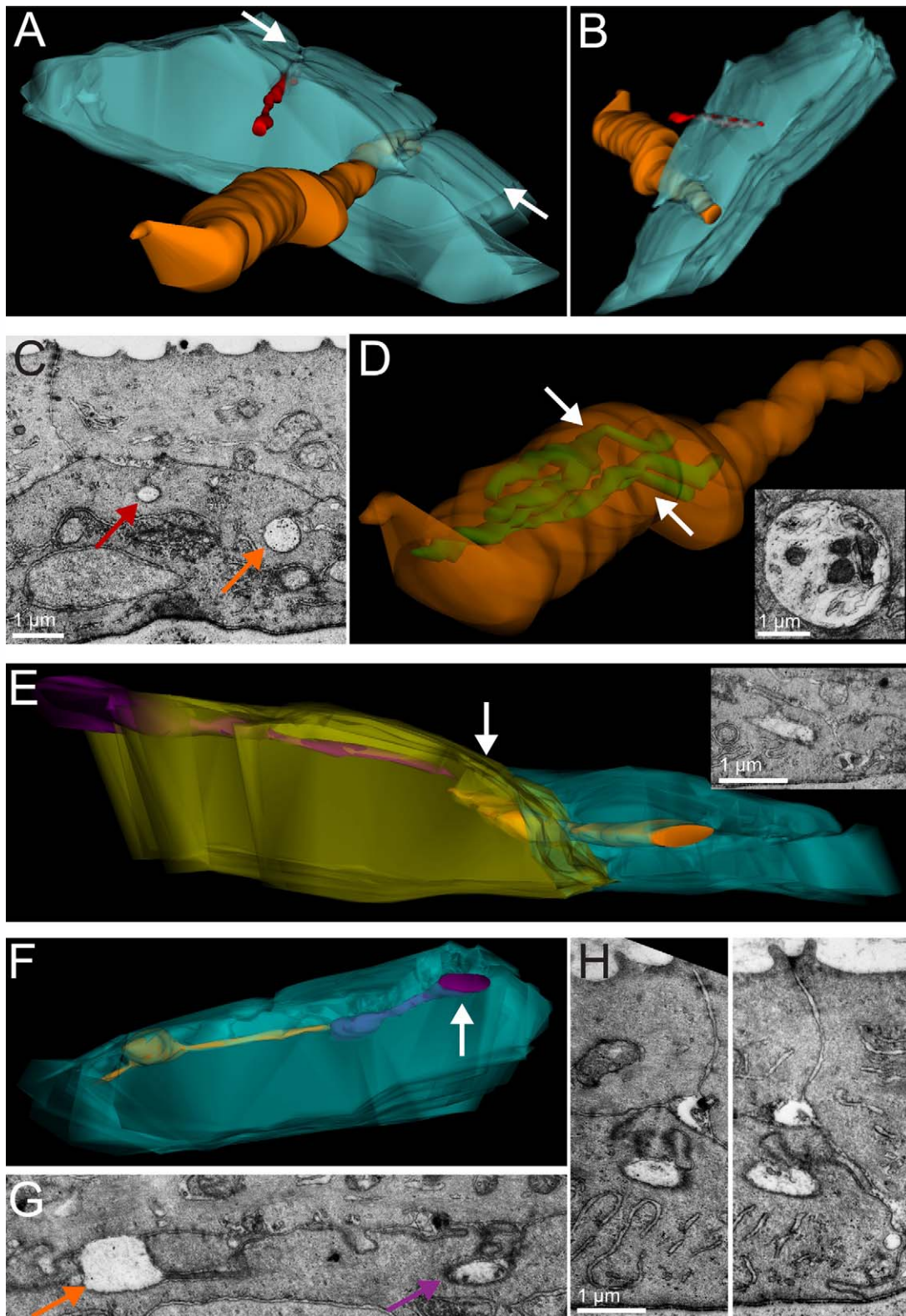


Figure 8

reached the skin, basal keratinocytes had not yet fully acquired their compact cuboidal shapes, secreted a distinct basement membrane, or formed extensive adhesive contacts with other keratinocytes. This less compact organization may facilitate the penetration of axons through the basal cell layer. Between 18 and 54 hpf, coinciding with the most intense arborization phase of trigeminal and RB axons (Sagasti et al., 2005), the basal skin layer became a well-organized epithelium with a prominent basement membrane. The appearance of the basement membrane was evident from our EM analysis and from staining embryos at 18 and 54 hpf with antilaminin (Fig. 2B) and antiheparin sulfate antibodies (not shown). Moore and Munger (1989) noted that a similar transition in the epithelial morphology of fetal human skin coincides with its innervation, prompting them to suggest that peripheral sensory axons might promote epithelial maturation (Moore and Munger, 1989). We tested this possibility by examining the ultrastructure of the skin in *ngn-1* morphant zebrafish, which lack primary somatosensory neurons (Andermann et al., 2002; Cornell and Eisen, 2002). In the absence of somatosensory neurons, basal cells matured normally, and a basement membrane formed at the appropriate stage, demonstrating that innervation is not required for this morphological transition to occur. In fact, in the absence of axons, more adhesive contacts formed between basal keratinocytes and peridermal cells, indicating that innervation loosened or delayed epithelial adhesion.

As larval development progresses, additional cell types appear in the zebrafish skin. For example, solitary chemosensory cells and ionocytes are found throughout the skin by 3 days postfertilization (Kotrschal et al., 1997; Hsiao et al., 2007; Jänicke et al., 2007). Additional cell types, including Merkel cells and mucus-secreting goblet cells, have been described in larval and adult zebrafish skin (Merrillees, 1974; Lane and Whitear,

1977; Kotrschal et al., 1993). By 78 hpf, our EM analyses revealed a variety of specialized cells within the epidermis, some of which appeared to be associated with axons (data not shown). Neuromasts, mechanosensory organs that are innervated by lateral line neurons, were apparent in our TEM images starting at 78 hpf. Cells likely to be solitary chemosensory cells were present by 54 hpf. By 78 hpf, cells resembling Merkel cells appeared between the periderm and the basal keratinocyte layers. Axons associated with these structures may represent the first population of specialized endings to innervate the skin. Perhaps the axons innervating these nascent Merkel cells belong to the *ngn-1*-independent population of mechanosensors that has been reported to form after the initial wave of neurogenesis (Caron et al., 2008).

Our observations raise questions about how the simple larval innervation pattern is transformed into the more complex adult arrangement. We did not detect significant RB death by 96 hpf either with our EM analyses or by following neurons over time with transgenic reporter lines, but it has been widely documented that zebrafish RB neurons die during larval development and that their function is taken over by DRG neurons (see, e.g., Reyes et al., 2004). Therefore, the mature larval and adult skin must accommodate later waves of axonal innervation. Adult skin innervation in teleost fish is more diverse than in larvae, consisting of axons that innervate specialized dermal structures, such as Merkel cells (Lane and Whitear, 1977), as well as free endings similar to those we observed in embryos and larvae (Whitear, 1971). Some of these adult free endings have been observed in the outer layers of the pseudostratified epidermis (Whitear, 1971), suggesting that newly innervating axons must penetrate through the basement membrane and several layers of tightly connected keratinocytes to reach these outer layers.

**Figure 8.** Serial section SEM reconstructions reveal that axons tunnel for long distances within basal skin cells at 78 hpf. **A:** 3-D reconstruction of 4.55  $\mu\text{m}$  of serial ultrathin sections. The basal skin cell (blue) is only partially reconstructed to reveal axon structure. Two axons are enveloped within the basal cell (red and orange). The orange axon was present in all sections and varied in diameter from 0.4 to 2  $\mu\text{m}$  before terminating in the final section. **B:** Same as in A, shown from an apical view. **C:** A single SEM section, from the location indicated with arrows in A. Red and orange arrows point to enveloped axon profiles of the red and orange axons reconstructed in A. **D:** Same orange axon as in A, made transparent to reveal the presence of reticular mitochondria inside the axon. Arrows indicate the location of the single SEM section shown in the *inset*. **E:** 3-D reconstruction of 1.68  $\mu\text{m}$  of serial ultrathin sections. Two basal skin cells (yellow and blue) engulf two axons (purple and orange), which travel longitudinally through the basal cells. The orange axon crosses between the two basal skin cells while remaining continuously enveloped. Arrow indicates the location of the single SEM section shown in the *inset*. **F:** 3-D reconstruction of 1.61  $\mu\text{m}$  of serial ultrathin sections. A single basal skin cell (blue) envelops two axons (purple and orange), which travel longitudinally through the basal cell. The orange axon has a large varicosity, shown in single SEM section in G. Orange and purple arrows point to membranes of the orange and purple axons reconstructed in F. **H:** Two serial SEM sections of the purple axon (arrow in F) show that the convoluted skin cell membrane channel that envelops the axon comes from different sides of the basal cell as the axon approaches the basal cell boundary. To view the reconstructions presented in these figures from multiple angles, movies showing 360° rotations of each reconstruction can be found at the website <http://www.mcdb.ucla.edu/Research/Sagasti/3Drotations>. Scale bars = 1  $\mu\text{m}$ .

## Basal keratinocytes envelop peripheral sensory axons

Our most surprising observation was that, by 78 hpf, many peripheral axons were tightly enveloped by basal skin cells. sSEM reconstruction from sections on coverslips revealed that enveloped axons tunneled over considerable distances through skin cells and crossed from one keratinocyte to another, in much the same way that a chain of Schwann cells envelops the primary axons of peripheral sensory neurons. These enveloped axons were much less common at 54 hpf, so they could arise from a later wave of differentiating neurons, perhaps the *ngn-1*-independent population (Caron et al., 2008), or they might be the same axons observed between the skin layers at 54 hpf that have progressively become enveloped. We favor the latter possibility, because, as the number of enveloped axons increased, correspondingly fewer axons were observed between the two skin layers.

Though unexpected, the envelopment of somatosensory axons by skin cells is not unique. For example, the mechanosensory ALM axons in *C. elegans* initially project between muscle cells and hypodermis but later become enveloped by the hypodermis (Chalfie and Sulston, 1981). Similar structures have been observed in outer layers of adult fish and human skin (Whitear, 1971; Cauna, 1973; Whitear and Moate, 1998), suggesting that this arrangement is a common feature of at least one class of peripheral sensory axons. In all of these cases, the membranes of the enveloped axon and keratinocyte are very tightly apposed to one another, adhesive junctions in the keratinocytes seal the channel between the axon and the outside of the skin cell, and electron-dense material in the skin cell surrounds the enveloped axons. These features are similar to those of nonmyelinating Schwann cells that ensheath the primary branches of peripheral axons (e.g., Cauna, 1973; Breathnach, 1977). Thus, by analogy to the function of Schwann cells, keratinocytes may provide mechanical support to axon free endings or regulate their conductance. It has also been suggested that keratinocytes might be primary sensors of thermosensory stimuli and communicate chemically with axonal free endings in the skin (Lee and Caterina, 2005). The tight apposition of enveloped free endings with surrounding keratinocytes would make these structures ideal candidates for such keratinocyte-to-axon sensory transmission.

## ACKNOWLEDGMENTS

We thank members of the Sagasti laboratory for comments on the manuscript, Sandhiya Kalyanasundaram for initial analysis of the keratin4:dsRED transgene, Majid Husain for making the keratin4:dsRED transgenic line,

Marriane Cilluffo for technical help with electron microscopy, and Jon Sack for computer access.

## LITERATURE CITED

- Andermann P, Ungos J, Raible DW. 2002. Neurogenin1 defines zebrafish cranial sensory ganglia precursors. *Dev Biol* 251: 45–58.
- Breathnach AS. 1977. Electron microscopy of cutaneous nerves and receptors. *J Invest Dermatol* 69:8–26.
- Caron SJ, Prober D, Choy M, Schier AF. 2008. In vivo birthdating by BAPTISM reveals that trigeminal sensory neuron diversity depends on early neurogenesis. *Development* 135:3259–3269.
- Cauna N. 1973. The free penicillate nerve endings of the human hairy skin. *J Anat* 115:277–288.
- Chalfie M, Sulston J. 1981. Developmental genetics of the mechanosensory neurons of *Caenorhabditis elegans*. *Dev Biol* 82:358–370.
- Cornell RA, Eisen JS. 2002. Delta/Notch signaling promotes formation of zebrafish neural crest by repressing neurogenin 1 function. *Development* 129:2639–2648.
- Costa ML, Escalera RC, Jazenko F, Mermelstein CS. 2008. Cell adhesion in zebrafish myogenesis: distribution of intermediate filaments, microfilaments, intracellular adhesion structures and extracellular matrix. *Cell Motil Cytoskeleton* 65:801–815.
- Davies A, Lumsden A. 1984. Relation of target encounter and neuronal death to nerve growth factor responsiveness in the developing mouse trigeminal ganglion. *J Comp Neurol* 223:124–137.
- Davies SN, Kitson DL, Roberts A. 1982. The development of the peripheral trigeminal innervation in *Xenopus* embryos. *J Embryol Exp Morphol* 70:215–224.
- Dubin AE, Patapoutian A. 2010. Nociceptors: the sensors of the pain pathway. *J Clin Invest* 120:3760–3772.
- Gong Z, Ju B, Wang X, He J, Wan H, Sudha PM, Yan T. 2002. Green fluorescent protein expression in germ-line transmitted transgenic zebrafish under a stratified epithelial promoter from keratin8. *Dev Dyn* 223:204–215.
- Goodman MB. 2006. Mechanosensation. *WormBook*, p 1–14.
- Harris KM, Perry E, Bourne J, Feinberg M, Ostroff L, Hurlbut J. 2006. Uniform serial sectioning for transmission electron microscopy. *J Neurosci* 26:12101–12103.
- Hayes BP, Roberts A. 1983. The anatomy of two functional types of mechanoreceptive “free” nerve-ending in the head skin of *Xenopus* embryos. *Proc R Soc Lond B Biol Sci* 218: 61–76.
- Higashijima S, Hotta Y, Okamoto H. 2000. Visualization of cranial motor neurons in live transgenic zebrafish expressing green fluorescent protein under the control of the islet-1 promoter/enhancer. *J Neurosci* 20:206–218.
- Hsiao CD, You MS, Guh YJ, Ma M, Jiang YJ, Hwang PP. 2007. A positive regulatory loop between foxi3a and foxi3b is essential for specification and differentiation of zebrafish epidermal ionocytes. *PLoS One* 2:e302.
- Jänicke M, Carney TJ, Hammerschmidt M. 2007. Foxi3 transcription factors and Notch signaling control the formation of skin ionocytes from epidermal precursors of the zebrafish embryo. *Dev Biol* 307:258–271.
- Kennedy WR, Wendelschafer-Crabb G. 1993. The innervation of human epidermis. *J Neurol Sci* 115:184–190.
- Kimmel CB, Westerfield M. 1990. Primary neurons of the zebrafish. In: Edelman GM, Gall WE, Cowan MW, editors. *Signal and sense*. New York: Wiley-Liss. p 561–588.
- Kitson DL, Roberts A. 1983. Competition during innervation of embryonic amphibian head skin. *Proc R Soc Lond B Biol Sci* 218:49–59.

- Kotrschal K, Whitear M, Finger TE. 1993. Spinal and facial innervation of the skin in the gadid fish *Ciliata mustela* (Teleostei). *J Comp Neurol* 331:407–417.
- Kotrschal K, Krautgartner WD, Hansen A. 1997. Ontogeny of the solitary chemosensory cells in the zebrafish, *Danio rerio*. *Chem Senses* 22:111–118.
- Kruger L, Light AR, Schweizer FE. 2003. Axonal terminals of sensory neurons and their morphological diversity. *J Neurocytol* 32:205–216.
- Kucenas S, Soto F, Cox JA, Voigt MM. 2006. Selective labeling of central and peripheral sensory neurons in the developing zebrafish using P2X<sub>3</sub> receptor subunit transgenes. *Neuroscience* 138:641–652.
- Lane EB, Whitear M. 1977. On the occurrence of Merkel cells in the epidermis of teleost fishes. *Cell Tissue Res* 182:235–246.
- Le Guellec D, Morvan-Dubois G, Sire JY. 2004. Skin development in bony fish with particular emphasis on collagen deposition in the dermis of the zebrafish (*Danio rerio*). *Int J Dev Biol* 48:217–231.
- Lee H, Caterina MJ. 2005. TRPV channels as thermosensory receptors in epithelial cells. *Pflügers Arch* 451:160–167.
- Lumpkin EA, Caterina MJ. 2007. Mechanisms of sensory transduction in the skin. *Nature* 445:858–865.
- Marmigère F, Ernfors P. 2007. Specification and connectivity of neuronal subtypes in the sensory lineage. *Nat Rev Neurosci* 8:114–127.
- Martin SC, Marazzi G, Sandell JH, Heinrich G. 1995. Five Trk receptors in the zebrafish. *Dev Biol* 169:745–758.
- Martin SC, Sandell JH, Heinrich G. 1998. Zebrafish TrkC1 and TrkC2 receptors define two different cell populations in the nervous system during the period of axonogenesis. *Dev Biol* 195:114–130.
- Martin SM, O'Brien GS, Portera-Cailliau C, Sagasti A. 2010. Wallerian degeneration of zebrafish trigeminal axons in the skin is required for regeneration and developmental pruning. *Development* 137:3985–3994.
- Merrilees MJ. 1974. Epidermal fine structure of the teleost *Esox americanus* (Esocidae, Salmoniformes). *J Ultrastruct Res* 47:272–283.
- Micheva KD, O'Rourke N, Busse B, Smith SJ. 2010. Array tomography: high-resolution three-dimensional immunofluorescence. *Cold Spring Harbor Protoc* 2010:top89.
- Moore SJ, Munger BL. 1989. The early ontogeny of the afferent nerves and papillary ridges in human digital glabrous skin. *Brain Res Dev Brain Res* 48:119–141.
- O'Brien GS, Rieger S, Martin SM, Cavanaugh AM, Portera-Cailliau C, Sagasti A. 2009. Two-photon axotomy and time-lapse confocal imaging in live zebrafish embryos. *J Vis Exp* 24:1129. doi: 10.3791/1129.
- Olsson C, Holmberg A, Holmgren S. 2008. Development of enteric and vagal innervation of the zebrafish (*Danio rerio*) gut. *J Comp Neurol* 508:756–770.
- Parsons MJ, Pollard SM, Saúde L, Feldman B, Coutinho P, Hirst EM, Stemple DL. 2002. Zebrafish mutants identify an essential role for laminins in notochord formation. *Development* 129:3137–3146.
- Pittman AJ, Law MY, Chien CB. 2008. Pathfinding in a large vertebrate axon tract: isotypic interactions guide retinotectal axons at multiple choice points. *Development* 135:2865–2871.
- Prober DA, Zimmerman S, Myers BR, McDermott BM, Kim SH, Caron S, Rihel J, Solnica-Krezel L, Julius D, Hudspeth AJ, Schier AF. 2008. Zebrafish TRPA1 channels are required for chemosensation but not for thermosensation or mechanosensory hair cell function. *J Neurosci* 28:10102–10110.
- Reyes R, Haendel M, Grant D, Melancon E, Eisen JS. 2004. Slow degeneration of zebrafish Rohon-Beard neurons during programmed cell death. *Dev Dyn* 229:30–41.
- Roberts A. 1980. The function and role of two types of mechanoreceptive “free” nerve endings in the head skin of amphibian embryos. *J Comp Physiol* 135:341–348.
- Roberts A, Blight AR. 1975. Anatomy, physiology and behavioural rôle of sensory nerve endings in the cement gland of embryonic *Xenopus*. *Proc R Soc Lond B Biol Sci* 192:111–127.
- Roberts A, Hayes BP. 1977. The anatomy and function of “free” nerve endings in an amphibian skin sensory system. *Proc R Soc Lond B Biol Sci* 196:415–429.
- Roberts A, Taylor JS. 1982. A scanning electron microscope study of the development of a peripheral sensory neurite network. *J Embryol Exp Morphol* 69:237–250.
- Sagasti A, Guido MR, Raible DW, Schier AF. 2005. Repulsive interactions shape the morphologies and functional arrangement of zebrafish peripheral sensory arbors. *Curr Biol* 15:804–814.
- Saint-Amant L, Drapeau P. 1998. Time course of the development of motor behaviors in the zebrafish embryo. *J Neurobiol* 37:622–632.
- Slatter CA, Kanji H, Coutts CA, Ali DW. 2005. Expression of PKC in the developing zebrafish, *Danio rerio*. *J Neurobiol* 62:425–438.
- Taylor JS, Roberts A. 1983. The early development of the primary sensory neurones in an amphibian embryo: a scanning electron microscope study. *J Embryol Exp Morphol* 75:49–66.
- Thiéry G, Bernier J, Bergeron M. 1995. A simple technique for staining of cell membranes with imidazole and osmium tetroxide. *J Histochem Cytochem* 43:1079–1084.
- Whitear M. 1971. The free nerve endings in fish epidermis. *J Zool* 163:31–236.
- Whitear M, Moate R. 1998. Cellular diversity in the epidermis of *Raja clavata* (Chondrichthyes). *J Zool Lond* 246:275–285.